# Torque Dynamics Enhancement of Railway Traction Drives Using Scalar Control

Ahmed Fathy Abouzeid [ID]
*Dept. of Electrical Engineering*
*University of Oviedo*
Gijón, Spain
abouzeidahmed@uniovi.es

Juan Manuel Guerrero [ID]
*Dept. of Electrical Engineering*
*University of Oviedo*
Gijón, Spain
guerrero@uniovi.es

Iker Muniategui
*Traction systems*
*Ingeteam Power Technology*
Zamudio, Spain
iker.muniategui@ingeteam.com

Aitor Endemaño
*Traction systems*
*Ingeteam Power Technology*
Zamudio, Spain
aitor.endemano@ingeteam.com

David Ortega
*Traction systems*
*Ingeteam Power Technology*
Zamudio, Spain
David.Ortega@ingeteam.com

Fernando Briz [ID]
*Dept. of Electrical Engineering*
*University of Oviedo*
Gijón, Spain
fbriz@uniovi.es

*Abstract*—Traction systems for railway typically use rotor field-oriented control (RFOC) at low speeds, and scalar control at high speeds to overcome the deterioration of the current regulator performance in the overmodulation region. Well-known limitations of scalar control are the slow dynamic response due to the coupling between torque and flux, as well as the risk of overcurrents. While this is not a problem for normal operation, as fast torque variations are not required, there are specific operating conditions in which fast torque response of scalar control might be required. This would include adhesion control, torsional torque vibration mitigation and torque ripple cancellation for traction systems fed from ac catenaries without a 2F filter in the dc-link. This paper proposes a method to enhance the dynamic response of scalar control. The principles of the proposed method are derived from vector control concepts. While the method could be applied to any electric drive using scalar control, the discussion presented in this paper will be targeted towards high power railway traction drives.

*Index Terms*—Scalar V/F control; railway traction drives; induction motors; beatless control; torsional torque oscillations.

## I. INTRODUCTION

Voltage-Source Inverter-fed Induction Machines (VSI-IM) are the preferred choice in railway traction systems due to their robustness and the slip inherent to IM, which allows multiple motors to be fed from a single inverter [1], [2]. VSI-IM traction drive systems can be fed from different power sources. For the specific case of ac catenaries, a four-quadrant converter (4QC) is required to supply the VSI-IM dc link. The fact that the catenary is single-phase results in well-known power oscillations at twice the catenary voltage frequency (2F), which has to be considered for the design of the traction system.

Fig. 1 shows the main circuit elements for a single-driven axle of a high-performance locomotive fed from an ac catenary. High-performance locomotive drives control consists of two control layers; an inner control layer aimed to provide the desired torque $T_e^*$ and an outer control layer that oversees traction force $F_t^*$ which can comprise several functionalities
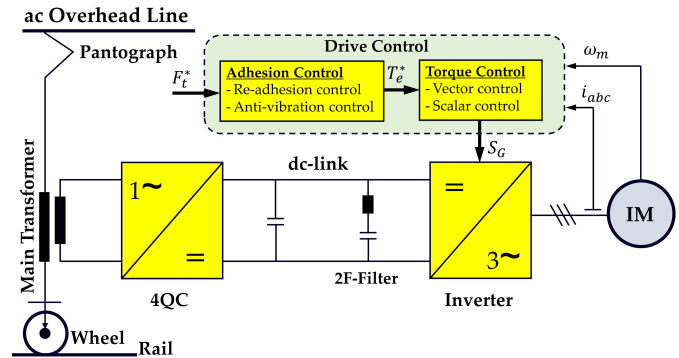


Fig. 1: Main circuit diagram for single driven axle of a high-performance locomotive.

as re-adhesion control, anti-slip control, torsional torque vibration mitigation, 2F oscillations cancellation, etc. Regarding the inner loop, RFOC with Pulse-Width Modulation/Space-Vector Modulation (PWM/SVM) is typically used at low-medium speeds, where the voltage margin and the switching to fundamental frequency ratio are sufficient for proper operation of the current regulators [3]. At high speeds, the lack of a voltage margin and the reduced switching to fundamental frequency ratio can seriously compromise the performance of FOC. Several attempts have been made to improve vector control performance in the overmodulation region, but this is at the price of increased complexity and parameter sensitivity, which has prevented their widespread use [4]–[6].

Scalar control is widely used when the drive operates close or at the voltage limit, constant V/F being the simplest implementation. Modulation strategies aimed to reduce switching losses and/or harmonic content are often used in this case [7]. Scalar control methods show slow torque dynamics due to the coupling between torque and flux and the need to prevent overcurrents. This is not a concern for normal operation of

traction drives. However, modern trains may require fast torque dynamics for advanced modes of operation, such as adhesion control, torsional torque vibration mitigation, and cancellation of torque ripple in traction drives fed from ac catenaries without an intermediate 2F filter (see Fig. 1) [8], [9].

Several methods aimed to improve the dynamic response of scalar control have been reported in the literature [10]–[15]. In [10], a feedforward term is added to the voltage magnitude command to compensate for the voltage variation caused by torque changes, which is claimed to decouple torque and flux and improve both the dynamic and steady-state response of the V/F control. Parameters required by the decoupling block change with the operating point. This involves the use of look-up tables which are built during a commissioning stage, what increases the complexity of the proposed method. In [13], [14], a transient voltage vector is estimated and added to the voltage vector command improving the transient response of the scalar V/F method. However, the estimated transient vector is obtained from d-q current regulators operating in parallel of the main V/F controllers which could be problematic when the machine enters the overmodulation region and the voltage margin required for the normal operation of the current controller is lost. Methods reported in [11], [12], [15] are targeted to overcome the limitations of scalar control at low fundamental frequencies only, being therefore disregarded.

In this paper, a method for enhancing the torque dynamics of scalar control when the drive operates at high fundamental frequencies in the overmodulation region, including six-step, is developed. The proposed method can potentially achieve dynamic responses comparable to those of vector controlled drives, but without the drawbacks of current regulators. The effectiveness of the proposed method will be validated through MATLAB/Simulink simulations in this paper. Construction of a test bench for experimental verification is ongoing.

## II. INDUCTION MOTOR MODEL

For the discussions following, variables in the stationary reference frame, stator voltage reference frame and rotor flux reference frame will be denoted by superscripts "$s$", "$slf$" and "$rf$" respectively.

The complex vector notation of an induction motor, with the stator current and the rotor flux as the state variables, are given by (1)-(2). $v_{dqs}^s$ denotes the stator voltage; $i_{dqs}^s$ is the stator current; $\hat{\lambda}_{dqr}^s$ represents the estimated rotor flux; $\hat{R}_s$ and $\hat{R}_r$ are the estimated stator and rotor resistances; $\hat{L}_s$, $\hat{L}_r$ and $\hat{L}_m$ are the estimated stator, rotor, and mutual inductances, respectively; $\omega_r$ is the rotor angular speed in electrical units; and $p$ is the derivative operator.

$$p i_{dqs}^s = \frac{1}{\hat{L}_{\sigma s}} \left( v_{dqs}^s - \hat{R}_s' i_{dqs}^s + \frac{\hat{L}_m}{\hat{L}_r} \omega_{br} \hat{\lambda}_{dqr}^s \right) \tag{1}$$

$$p \hat{\lambda}_{dqr}^s = \frac{\hat{L}_m}{\hat{L}_r} \hat{R}_r i_{dqs}^s - \omega_{br} \hat{\lambda}_{dqr}^s \tag{2}$$

where

$$\hat{R}_s' = \hat{R}_s + \hat{R}_r \left( \frac{\hat{L}_m}{\hat{L}_r} \right)^2 \;\; ; \;\; \hat{L}_{\sigma s} = \hat{L}_s - \frac{\hat{L}_m^2}{\hat{L}_r} \; ; \omega_{br} = \frac{\hat{R}_r}{\hat{L}_r} - j\omega_r$$

$\hat{R}_s'$ and $\hat{\sigma}$ are the estimated stator transient resistance and leakage inductance respectively. The electromagnetic torque $T_e$ is given by (3) in terms of stator current and rotor flux where $P$ is the pole-pairs.

$$T_e = \frac{3}{2} P \frac{\hat{L}_m}{\hat{L}_r} \left( \hat{\lambda}_{dr}^s i_{qs}^s - \hat{\lambda}_{qr}^s i_{ds}^s \right) \tag{3}$$

By aligning the $d$-axis of the rotating reference frame with the rotor flux, i.e., $\hat{\lambda}_{dqr}^{rf} = \hat{\lambda}_{dr}^{rf} = \hat{\lambda}_r$ , the stator voltage and the stator flux equations become (4) and (5), where $\omega_e$ is the angular speed in electrical units of the synchronous reference frame.

$$v_{dqs}^{rf} = \hat{R}_s' i_{dqs}^{rf} + p \hat{\lambda}_{dqs}^{rf} + j\omega_e \hat{\lambda}_{dqs}^{rf} \tag{4}$$

$$\hat{\lambda}_{dqs}^{rf} = \frac{\hat{L}_m}{\hat{L}_r} \hat{\lambda}_{dqr}^{rf} + \hat{L}_{\sigma s} i_{dqs}^{rf} \tag{5}$$

## III. VECTOR VS. SCALAR CONTROL

Vector control uses the dynamic equations of the machine to achieve decoupled control of torque and flux (see Fig. 2a). This allows to fully exploit machine torque capability without surpassing machine or power converter current limits. On the contrary, open-loop scalar V/F control schemes make the stator voltage magnitude proportional to the frequency, leading to an almost constant flux in the machine. Nevertheless, there is a number of issues e.g. incorrect voltage to frequency ratios, voltage drops in the stator resistance, or variations of the inverter dc-link voltage, etc. which could drift the actual operating point from the desired value. To overcome these effects, the performance of V/F control can be improved with the addition of feedback loops [16].

Closed-loop V/F control has been widely used in traction drives. Flux and the torque are regulated in this case using Proportional-Integral (PI) controllers. This closed-loop scheme is known as slip/flux scalar V/F control (SLF), (see Fig. 2b), which consists of two terms: 1) the first term provides the base value of the stator voltage magnitude through the V/F characteristic, with adapting the rotor flux level through a PI regulator. 2) the second term provides the base value for the slip, then the torque is controlled by regulating the slip with no error [7]. Closed-loop V/F control is usually applied at high speed operation where power converter operates close to its voltage limit, including overmodulation and six-step [3]. This enables precise control of the machines' operating point in steady-state avoiding the deterioration of the current regulators due to the generated harmonic components of the machine current during the over-modulation. However, closed-loop V/F schemes have slower dynamic response compared to rotor flux field-oriented control (RFOC). Since the voltage magnitude and phase angle commands are independently obtained, both flux and torque controllers must be tuned for relatively low bandwidths to avoid cross-coupling interactions.
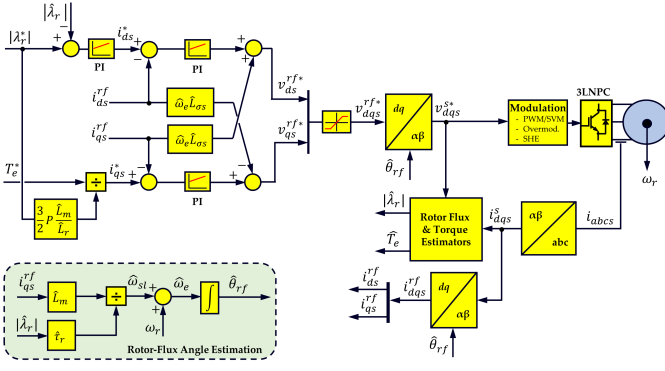
(a)
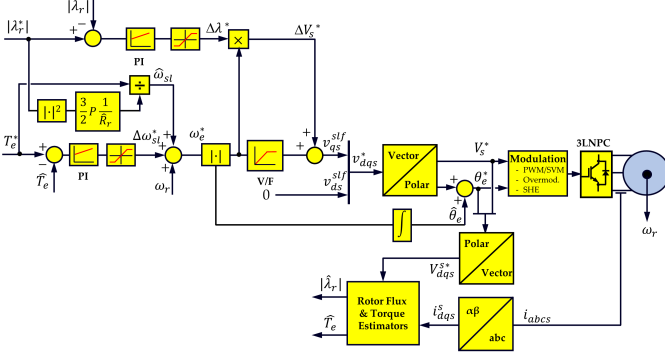


(b)

Fig. 2: Block diagram of closed-loop control scheme for induction motors: a) Rotor flux field-oriented control (RFOC); b) Stator voltage oriented V/F with slip & flux control (SLF).

## IV. SCALAR CONTROL WITH ENHANCED DYNAMICS

The following discussion assumes that the induction machine in Fig. 2 is operating at relatively high speed. The $q$-axis of the synchronous reference is defined to be aligned with the stator voltage vector (6b). If a sudden change in the torque command is applied, the slip angular speed $\hat{\omega}_{sl}$ will increase proportionally (see Fig. 2b), increasing therefore the angular speed of the stator voltage vector. The magnitude of the stator voltage $v_{qs}^{slf}$ will also increase according to the predefined V/Hz ratio to keep the flux constant. Such sudden changes of the stator voltage angle and magnitude can result in large transient currents. Due to this, the rate of variation of the torque command, i.e. the dynamic response of the scalar control, must be limited.

$$\begin{cases} v_{ds}^{slf} & = 0 & \text{(6a)} \\ v_{qs}^{slf} & = V_s^* = |\hat{R}_s I_s + j\hat{\omega}_e \hat{\lambda}_s| \cong |\hat{\omega}_e \hat{\lambda}_s| & \text{(6b)} \end{cases}$$

To understand how the dynamic response of the scalar control can be enhanced, it is useful to analyze the behavior of the stator voltage from a rotor flux oriented control perspective. Using (5) and (4), it is possible rewrite (6a) and (6b) in a rotor
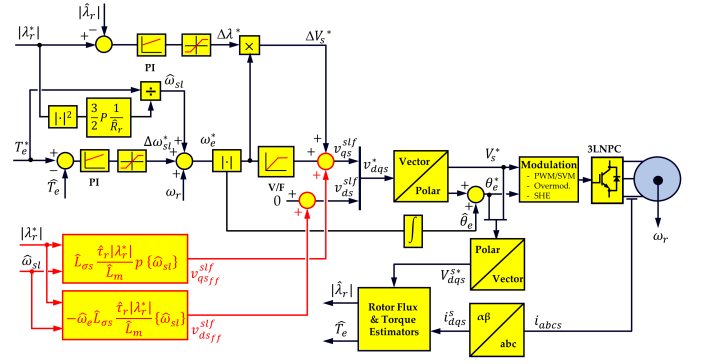


Fig. 3: Proposed feedforward compensation for stator voltage oriented scalar V/F control.

flux reference frame (7a) and (7b).

$$\begin{cases} v_{ds}^{rf} & = \hat{R}_s' i_{ds}^{rf} + \hat{L}_{\sigma s} p i_{ds}^{rf} - \hat{\omega}_e \hat{L}_{\sigma s} i_{qs}^{rf} - \hat{R}_r \frac{\hat{L}_m}{\hat{L}_r^2} \hat{\lambda}_{dr}^{rf} & \text{(7a)} \\ v_{qs}^{rf} & = \hat{R}_s' i_{qs}^{rf} + \hat{L}_{\sigma s} p i_{qs}^{rf} + \hat{\omega}_e \hat{L}_{\sigma s} i_{ds}^{rf} + \hat{\omega}_r \frac{\hat{L}_m}{\hat{L}_r} \hat{\lambda}_{dr}^{rf} & \text{(7b)} \end{cases}$$

Equations (7a) and (7b) can be used to define feedforward terms aimed to improve the dynamic response of the scalar control in Fig. 2. Despite of its apparent complexity, and the associated parameter sensitivity, a number of simplifications are feasible: 1) The resistive voltage drops $\hat{R}_s' i_{ds}^{rf}$ and $\hat{R}_s' i_{qs}^{rf}$ can be neglected in high speed operation; 2) $\hat{L}_{\sigma s} p i_{ds}^{rf}$ equals zero assuming that the flux is kept constant; 3) $\hat{R}_r \frac{\hat{L}_m}{\hat{L}_r^2} \hat{\lambda}_{dr}^{rf}$ can be shown to be negligible as the rotor flux and rotor resistance values of high power machines are small compared to low power machines. The relationship between the stator voltage, $q$-axis current and flux can be then simplified as:

$$\begin{cases} v_{ds}^{rf} & \cong -\hat{\omega}_e \hat{L}_{\sigma s} i_{qs}^{rf} & \text{(8a)} \\ v_{qs}^{rf} & \cong \hat{L}_{\sigma s} p i_{qs}^{rf} + \hat{\omega}_e \hat{L}_{\sigma s} i_{ds}^{rf} + \hat{\omega}_r \frac{\hat{L}_m}{\hat{L}_r} \hat{\lambda}_{dr}^{rf} & \text{(8b)} \end{cases}$$

Equation (8a) shows the feedforward term to be added to the $d$-axis voltage component $v_{ds}^{rf}$ to take into account changes in the torque (i.e. $q$-axis current). The transient response improvement is achieved by the $\hat{L}_{\sigma s} p i_{qs}^{rf}$ term of the stator voltage $q$-axis component in (8b). This term is a function of the $q$-axis current derivative and enhances therefore torque dynamic behavior. Since this action must be applied to the scalar control, the $q$-axis current is transformed into the slip angular speed using (9).

$$\hat{\omega}_{sl} = \frac{\hat{L}_m}{\hat{\tau}_r |\lambda_r^*|} i_{qs}^{rf} \quad \text{(9)}$$

Finally, the feedforward terms aimed to improve the dynamic response are given in (10a)&(10b) by substituting (9) in (8a)&(8b), where the steady-state value is nearly achieved from the V/F relation, i.e. $|\hat{\omega}_e \hat{\lambda}_s| \cong \hat{\omega}_e \hat{L}_{\sigma s} i_{ds}^{rf} + \hat{\omega}_r \frac{\hat{L}_m}{\hat{L}_r} \hat{\lambda}_{dr}^{rf}$ in (6b). Fig. 3 shows the block diagram of the proposed method.

$$\begin{cases} v_{ds_{ff}}^{slf} & \cong -\hat{\omega}_e \hat{L}_{\sigma s} \frac{\hat{\tau}_r |\lambda_r^*|}{\hat{L}_m} \hat{\omega}_{sl} & \text{(10a)} \\ v_{qs_{ff}}^{slf} & \cong \hat{L}_{\sigma s} \frac{\hat{\tau}_r |\lambda_r^*|}{\hat{L}_m} p \hat{\omega}_{sl} & \text{(10b)} \end{cases}$$
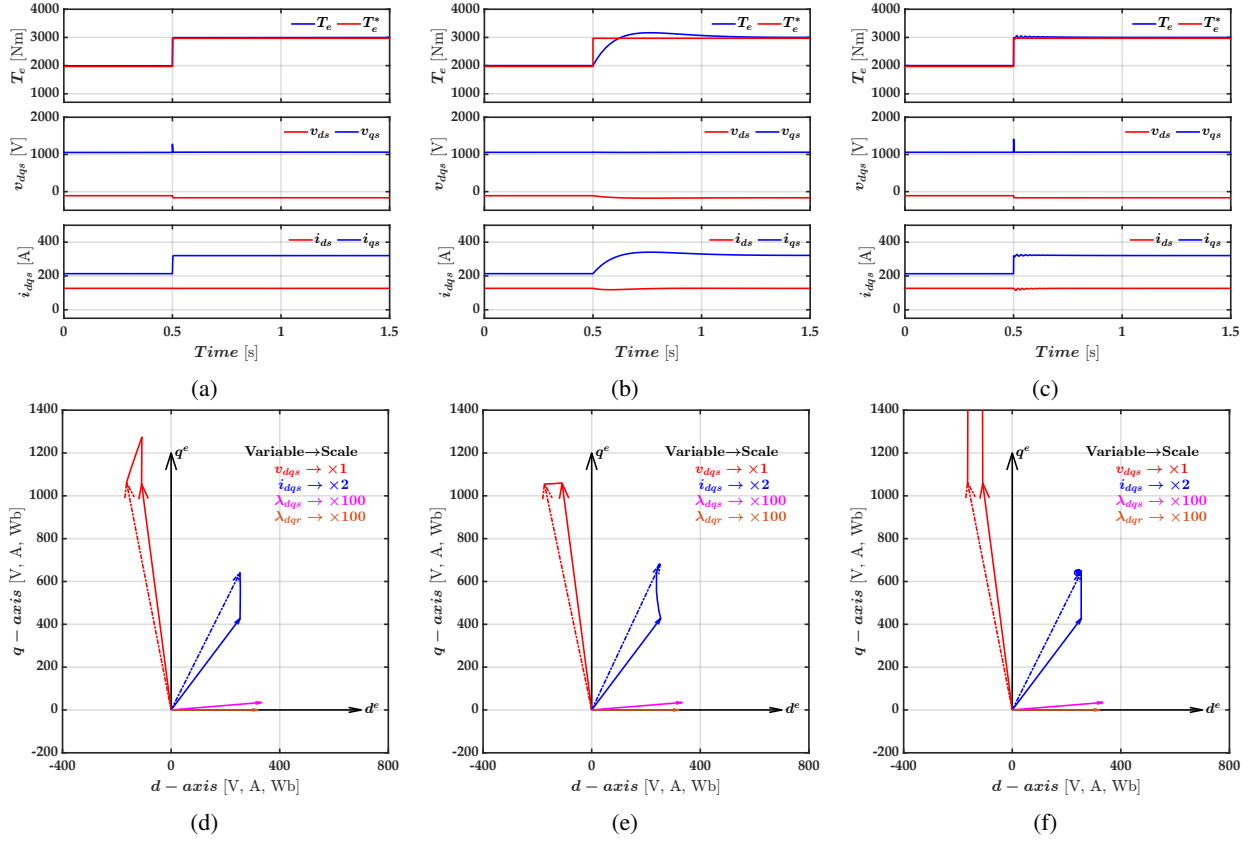
Fig. 4: Response to a torque command step change: (a), (d) RFOC; (b), (e) SLF; (c), (f) SLF with full feedforward terms. Top: time response. Bottom: vector trajectories. Solid vector: starting position. Dashed vector: steady-state position.

## V. SIMULATION RESULTS

The performance of the proposed method has been validated by simulation using MATLAB/Simulink. The induction motor parameters at base speed are given in Table I. The dynamic response of the proposed method is validated first with the IM connected to an ideal (linear) voltage. Further a Three-Level Neutral-Point-Clamped (3LNPC) inverter will be used. Usually high-power traction drives operate with low switching frequencies to reduce switching losses, Space-Vector PWM (SVPWM) with a switching frequency of 1 kHz will be used. An infinite inertia is assumed; consequently, the rotor speed remains constant. This assumption is realistic in railway traction drives during short periods of time due to train inertia.

TABLE I: Specifications of the induction motor and nominal values at base speed

| Variable | Value | Unit |
|---|---|---|
| DC-link voltage | 3600 | V |
| Rated Power | 1084 | kW |
| Rated Voltage ($V_{LL}$, rms) | 2727 | V |
| Pole-pairs ($P$) | 2 | Poles |
| Stator resistance ($R_s$) | 55.38 | mΩ |
| Stator inductance ($L_s$) | 26.45 | mH |
| Torque | 3241 | Nm |
| Speed | 3194 | rpm |

Fig. 4 shows the response to a torque step from 2 kNm

to 3 kNm of RFOC (Fig. 2a), scalar control (SLF) (Fig. 2b), and scalar control (SLF) with both $dq$-axis feedforward terms (Fig. 3). Top subfigures show the torque, stator voltage and current vectors response in the time domain while bottom subfigures show the vector diagrams. For the sake of comparison, all vector diagrams are shown in the rotor-flux reference frame.

The superior dynamic performance of RFOC over scalar control is readily observed from Fig. 4a and Fig. 4b. The differences in the trajectories followed by the voltage in Fig. 4d and Fig. 4e explain this behavior. For the RFOC case, current controllers force the current to move along the $q$-axis, while for the scalar control case, a deviation from the desired trajectory is observed. Adding the $d$-axis feedforward term is seen to improve the dynamic response providing the correct position of the stator voltage vector, but at the price of inadmissible torque and current oscillations. The dynamic response with only $d$-axis feedforward has been omitted as it provides an unsatisfactory response. Full feedforward (Fig. 4c and Fig. 4f) are seen to provide a dynamic response comparable to that of field-oriented control. However, it is seen the the stator voltage vector reached its limits. In practice, this behavior is undesired, but can be avoided by limiting the maximum slope of the torque command, which is a common practice in traction drives.

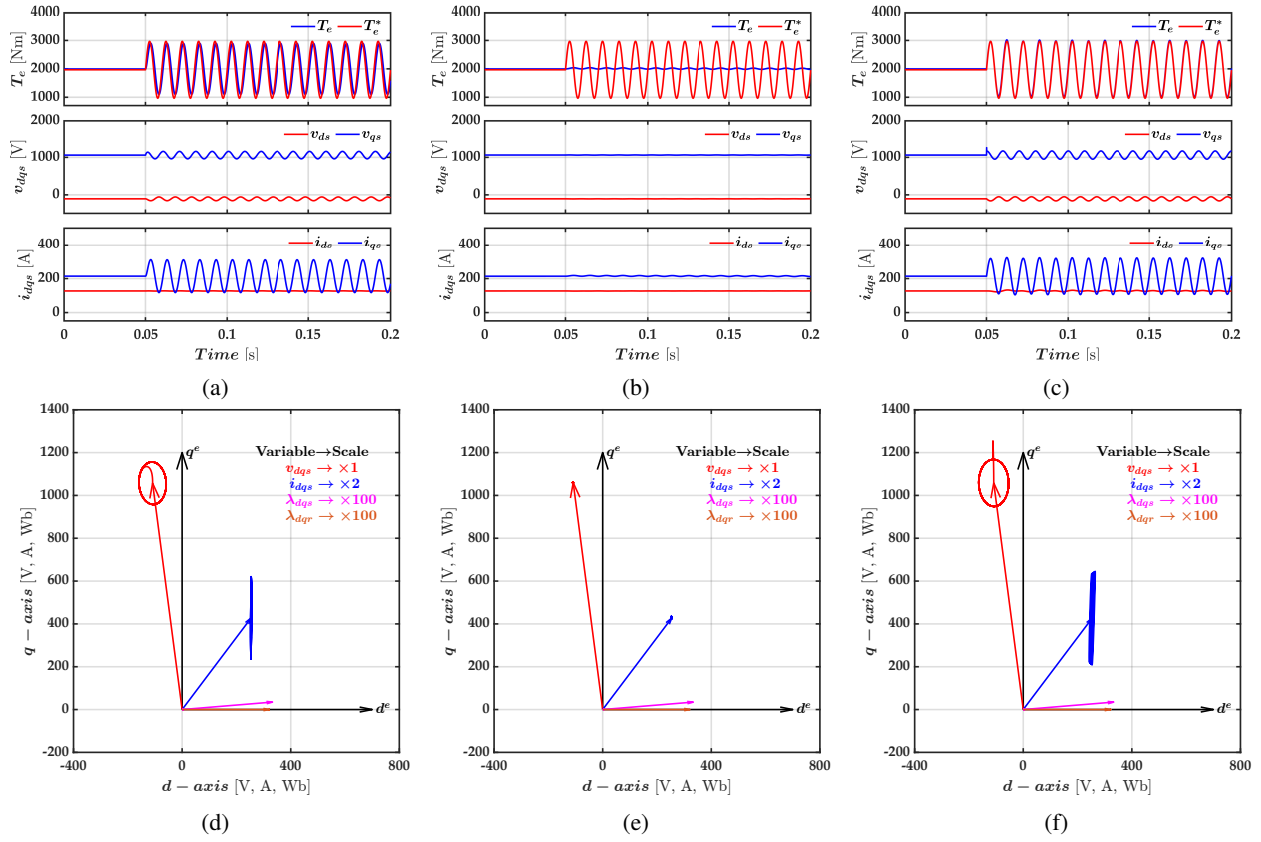While thew fast changes in the torque command shown

Fig. 5: Response to commanded torque oscillation at 100 Hz: (a), (d) RFOC; (b), (e) SLF; (c), (f) SLF with full feedforward terms. Top: time response. Bottom: vector trajectories. Solid vector: starting position. Dashed vector: steady-state position.

in Fig. 4 are not normally needed, there is a number of operating conditions in which they might be required. This would include to mitigate torque ripples produced by the 2F oscillation of the dc-link voltage in ac catenaries when a 2F filter is not used; to implement anti-slip control and for active cancellation of torsional torque vibrations. In all these case, the control should be able to produce torque oscillations at frequencies around twice the catenary frequency [17].

Fig. 5 shows the dynamic response of the control schemes under discussion subjected to a torque command oscillating at 100 Hz (which corresponds to 2F for 50 Hz catenaries). While RFOC (see Fig. 5a) precisely follows the torque command, SLF is unable to track such fast torque variations (see Fig. 5b). Use of full feedforward 5c) is seen to produce a dynamic response comparable fo the of RFOC.

All the simulation results shown so far used a linear voltage source. While useful for validation of the concepts, the use of the linear voltage source hides effects as the now due to commutation and the delays intrinsic to PWM which can play a relevant role in the real system. The proposed method has also also been validated when feeding the IM from a 3LNPC, as shown in Fig. 6. A step of 2 kNm is applied at $t = 0.5$s then a ramp of 1 kNm is applied at $t = 1.5$s (see Fig. the left column of Fig. 6).
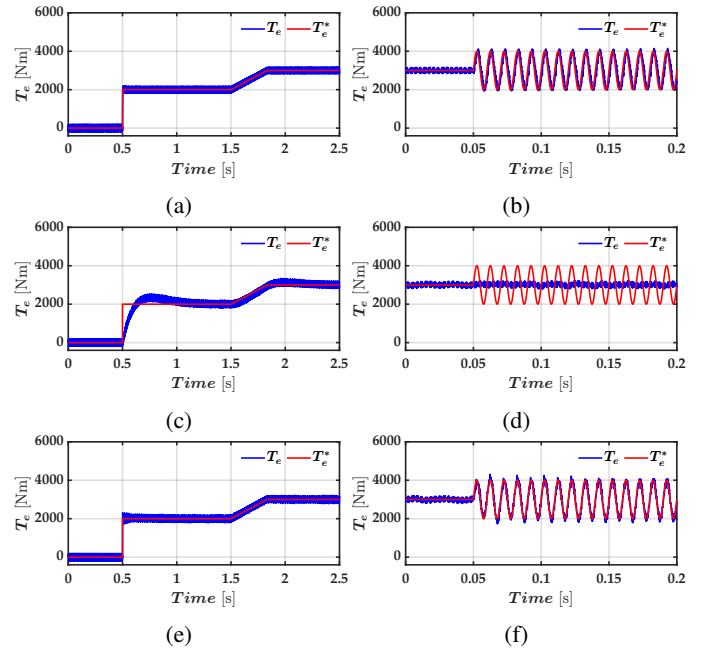


Fig. 6: Response of IM connected to 3LNPC: (a), (b) RFOC; (c), (d) SLF; (e), (f) SLF with full feedforward terms. Left: with step/ramp torque command. Right: with 100 Hz injected oscillation torque command.

The maximum allowable torque gradient will depend on each application. A 3 kNm/s has been chosen for the machine considered in this paper. The torque oscillation injection results are shown in the right column of Fig. 6. The results confirm the effectiveness of the proposed method.

## VI. Conclusions

This paper proposes a method to improve the dynamic response of electric drives using scalar control. The proposed method uses vector control concepts to obtain feedforward voltage terms to be applied to the scalar control, being suitable for its use with electric drives operating at high fundamental frequencies, and with high modulation indexes, including six-step.

The proposed methods can achieve a similar dynamic performance as RFOC. By this way, the deterioration of the RFOC current regulators performance operating at overmodulation range can be avoided without affecting the overall performance of the traction drive.

While the proposed concepts can be applied to any electric drive using scalar control, the specific application being considered are traction drives for railway. Potential uses would include mitigation of torque pulsations in ac catenaries for traction drives operating without 2F filter; anti-slip control and suppression of torsional torque vibrations.

Preliminary simulation results have been provided in this paper. Construction of the testbench for experimental validation is ongoing.

## References

[1] R. Hill, "Electric railway traction. ii. traction drives with three-phase induction motors," *Power Engineering Journal*, vol. 8, no. 3, pp. 143–152, 1994.

[2] A. M. El-Refaie, "Motors/generators for traction/propulsion applications: A review," *IEEE Vehicular Technology Magazine*, vol. 8, no. 1, pp. 90–99, 2013.

[3] T. H. Nguyen, T. L. Van, D.-C. Lee, J.-H. Park, and J.-H. Hwang, "Control mode switching of induction machine drives between vector control and v/f control in overmodulation range," *Journal of Power Electronics*, vol. 11, no. 6, pp. 846–855, 2011.

[4] Y. Kwon, S. Kim, and S. Sul, "Six-step operation of pmsm with instantaneous current control," *IEEE Transactions on Industry Applications*, vol. 50, no. 4, pp. 2614–2625, 2014.

[5] X. Fang, Z. Tian, H. Li, Z. Yang, F. Lin, and S. Hillmansen, "Current closed-loop control and field orientation analysis of an induction motor in six-step operation for railway applications," *IET Power Electronics*, vol. 12, no. 6, pp. 1462–1469, 2019.

[6] J. Holtz and N. Oikonomou, "Estimation of the fundamental current in low switching frequency high-dynamic medium voltage drives," in *2007 IEEE Industry Applications Annual Meeting*. IEEE, 2007, pp. 993–1000.

[7] A. Fathy Abouzeid, J. M. Guerrero, A. Endemaño, I. Muniategui, D. Ortega, I. Larrazabal, and F. Briz, "Control strategies for induction motors in railway traction applications," *Energies*, vol. 13, no. 3, p. 700, 2020.

[8] M. Fleischer and K. Kondo, "Slip-stick vibration suppression by modal state control for traction drive-trains," *IEEJ Journal of Industry Applications*, vol. 5, no. 1, pp. 1–9, 2016.

[9] B. Gou, X. Feng, W. Song, K. Han, and X. Ge, "Analysis and compensation of beat phenomenon for railway traction drive system fed with fluctuating dc-link voltage," in *Proceedings of The 7th International Power Electronics and Motion Control Conference*, vol. 1. IEEE, 2012, pp. 654–659.

[10] B. K. Bose, "Scalar decoupled control of induction motor," *IEEE transactions on industry applications*, no. 1, pp. 216–225, 1984.

[11] A. Smith, S. Gadoue, M. Armstrong, and J. Finch, "Improved method for the scalar control of induction motor drives," *IET Electric Power Applications*, vol. 7, no. 6, pp. 487–498, 2013.

[12] I. Boldea, A. Moldovan, and L. Tutelea, "Scalar v/f and i-f control of ac motor drives: An overview," in *2015 Intl Aegean Conference on Electrical Machines Power Electronics (ACEMP), 2015 Intl Conference on Optimization of Electrical Electronic Equipment (OPTIM) 2015 Intl Symposium on Advanced Electromechanical Motion Systems (ELECTROMOTION)*, 2015, pp. 8–17.

[13] S. R. P. Reddy and U. Loganathan, "Robust and high-dynamic-performance control of induction motor drive using transient vector estimator," *IEEE Transactions on Industrial Electronics*, vol. 66, no. 10, pp. 7529–7538, 2018.

[14] ——, "Improving the dynamic response of scalar control of induction machine drive using phase angle control," in *IECON 2018-44th Annual Conference of the IEEE Industrial Electronics Society*. IEEE, 2018, pp. 541–546.

[15] Z. Zhang and A. M. Bazzi, "Robust sensorless scalar control of induction motor drives with torque capability enhancement at low speeds," in *2019 IEEE International Electric Machines & Drives Conference (IEMDC)*. IEEE, 2019, pp. 1706–1710.

[16] B. Bose, "Modern power electronics and ac drives-prentice-hall," *Inc, Publication*, pp. 70–74, 2002.

[17] Y. Lei, K. Wang, L. Zhao, and Q. Ge, "An improved beatless control method of ac drives for railway traction converters," in *2016 19th International Conference on Electrical Machines and Systems (ICEMS)*. IEEE, 2016, pp. 1–5.